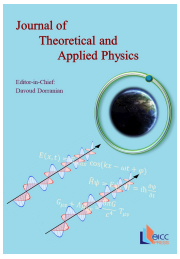

Volume 17, Issue 2, 172325 (1-6)

Journal of Theoretical and Applied Physics (JTAP)

https://dx.doi.org/10.57647/j.jtap.2023.1702.25

Electrodeposition of cobalt oxide thin films for potential applications

Augustine Sandra , Azubike Josiah Ekpunobi , Diemiruaye Mimi Jeroh *

Department of Physics and Industrial Physics, Nnamdi Azikiwe University, Awka, Nigeria.

***Corresponding author**: dm.jeroh@unizik.edu.ng

Received 30 December 2022; Accepted 26 February 2023; Published online 30 February 2023

Abstract:
Cobalt oxide thin films at varied molar concentrations were prepared by electrodeposition technique. Ultraviolet-Visible (UV/VIS) analysis conducted on the grown films revealed blue shift in the absorption edge at increased molar concentrations, which is a consequence of band gap widening. The band gap values (3.65 eV to 3.85 eV) in this research are greater than the value (2.4 eV) for the bulk phase of cobalt oxide. This increase in band gap can be likened to higher concentration effect and quantum-size phenomenon. Scanning Electron Microscopy (SEM) analysis indicated a porous nature for the material, suggesting its ability in absorbing ultraviolet (UV) radiation, thus confirming its use as an absorber material for solar cells fabrication. Energy Dispersive X-ray (EDX) study confirmed the growth of cobalt oxide. X-ray diffraction (XRD) analysis confirms the crystalline nature of the films with grain sizes within the range of 0.7 nm to 1 nm for varied molar concentrations. Electrical studies reveal a linear relationship of resistivity values with molar concentrations, while the conductivity values reveal inverse relationship with molar concentration.

Keywords: Molar concentrations; Cobalt oxide; Band widening; Blue-shift; Crystalline

1. Introduction

Semiconductor thin film research has continued to be an area of intense interest. This possibly stems from the fact that devices based on semiconductors have proven effective in diverse areas like solar cells (SCs) fabrication, fabricating electronic devices, fibre-optics technology, etc [1]. One essence of studying semiconductor films is to understand their various underlying properties and suggest applications based on these properties.
Cobalt oxide fall within the materials classified as transition metal oxides (TMOs) or transparent conducting oxides (TCOs). Due to their very good optical, electronic, catalytic and magnetic properties, TMOs are considered as promising materials for variety of technological applications [2]. These properties have triggered their use in optoelectronic devices such as electrochromic sensors and photovoltaic devices [3]. Cobalt oxide exhibit p-type conductivity and ferromagnetic behaviour.
Cobalt oxide, due to its power storage capacity, finds applications in supercapacitors and selective absorbers in solar cells. Cobalt oxides, due to their importance, also have applications in the manufacture of sensors, optoelectronics and other electrical devices [4]. Cobalt oxide has been synthesized hydrothermally [5], by sol-get coating [6], by electrochemical deposition [7–9] and pyrolysis [10].
In this research, novel cobalt oxide is prepared by electrodeposition at different molar concentrations. Increased molar concentration has shown to improve the crystalinity of the films [2]. Electrodeposition technique was preferred in this research when compared to other growth techniques of semiconductors due to its low cost. Electrodeposition has the advantage of scalability, simplicity and manufacturability [11]. Electrodeposition also offers the ability to control the composition of the chemical and film thickness by variation of either current or potential [12]. After deposition, the optical, electrical, and structural properties of the material were examined for possible applications of the material.

2. Materials and method

2.1 Materials

The starting chemicals and solvents include cobalt (II) chloride ($CoCl_2.6H_2O$), potassium hydroxide (KOH), ammonia solution (NH_3) and de-ionized water. Tin oxide substrates doped with fluorine (FTO) were employed for

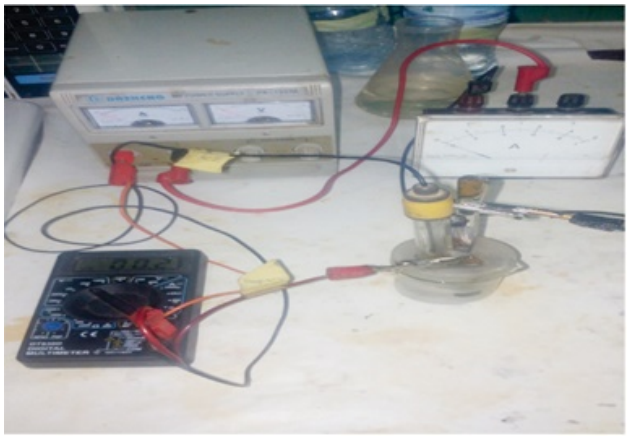

Figure 1. Pictorial representation of an electrodeposition setup.

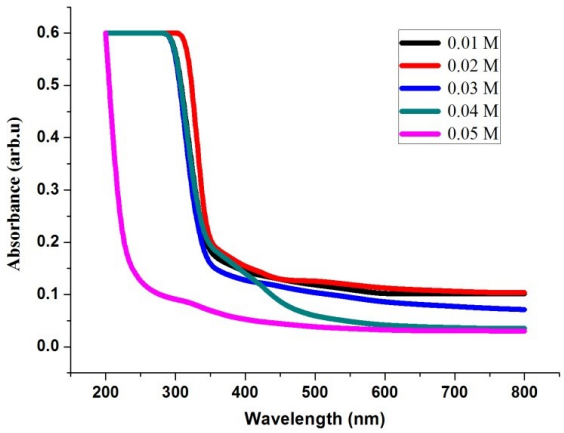

Figure 2. Absorption spectra of cobalt oxide prepared at different molar concentrations.

the deposition.

Power source

The power supply used in this work was a regulated power supply capable of converting AC voltage into DC voltage. The 220 AC voltage from the main was converted into 120 DC voltage using AC - DC converter. During connection, the positive terminal (live) of the output from the power supply was red while the negative (neutral) of the output from the power supply was black. The working electrode (FTO glass) was connected to the negative terminal (cathode) while the carbon electrode was connected to the positive terminal (anode) during the deposition. The pictorial representation of the experimental setup is displayed in Figure 1.

2.2 Method

Electrodeposition setup comprising two-electrode cell was employed for the film's growth. The electrochemical bath comprised a cation source ($CoCl_2.6H_2O$ for Co^{2+}), an anion source (KOH for OH^{2-}) and deionized water in a 100 ml beaker. The reaction bath was continuously stirred with a magnetic stirrer hot plate, while a DC voltage power source was applied as the source of electric field. In the setup, a conducting glass (FTO) served as cathode while carbon served as anode. With the setup in place, the concentration of the cation was varied at 0.01 mol, 0.02 mol, 0.03 mol, 0.04 mol, and 0.05 mol respectively while other growth parameters were kept constant.

The reaction equation is given as:

$$CoCl_2.6H_2O + KOH = Co(OH)_2 + 2KCL + 6H_2O$$

Details of the experimental procedure can be further explained using Table 1.

where A1, A2, A3, A4 and A5 are all Fluorine doped tine oxide substrate that was used for the deposition. In concentration variation, 25 ml of $CoCl_2.6H_2O$, 10 ml of KOH and 5 ml of NH_3 were measured into 100 ml beaker, concentration was varied at the range of 0.01 mol, 0.02 mol, 0.03 mol, 0.04 mol and 0.05 mol respectively at constant time 8 sec. and constant voltage 5 V.

2.3 Characterization of the films

Optical characterization was performed by a UV/1800 Visible Spectrophotometer, structural studies (X-ray diffraction) was obtained using a Bruker-D8 Advance X-ray diffractometer with Cu-Kα line ($\lambda = 1.54056\AA$) in 2θ scanning range from 10° - 70°, electrical characterization was performed using four point probe (Model T345) while Scanning Electron Microscopy (SEM) and Energy Dispersive Analysis (EDX) were used to obtain the surface morphology and compositions of the films respectively.

Table 1. Variation of concentration.

Slide No	$CoCl_2.6H_2O$ (ml)	KOH (ml)	NH_3 (ml)	Conc. (mol)	Time (Sec.)	Voltage (v)
A1	25	10	5	0.01	8	5
A2	25	10	5	0.02	8	5
A3	25	10	5	0.03	8	5
A4	25	10	5	0.04	8	5
A5	25	10	5	0.05	8	5

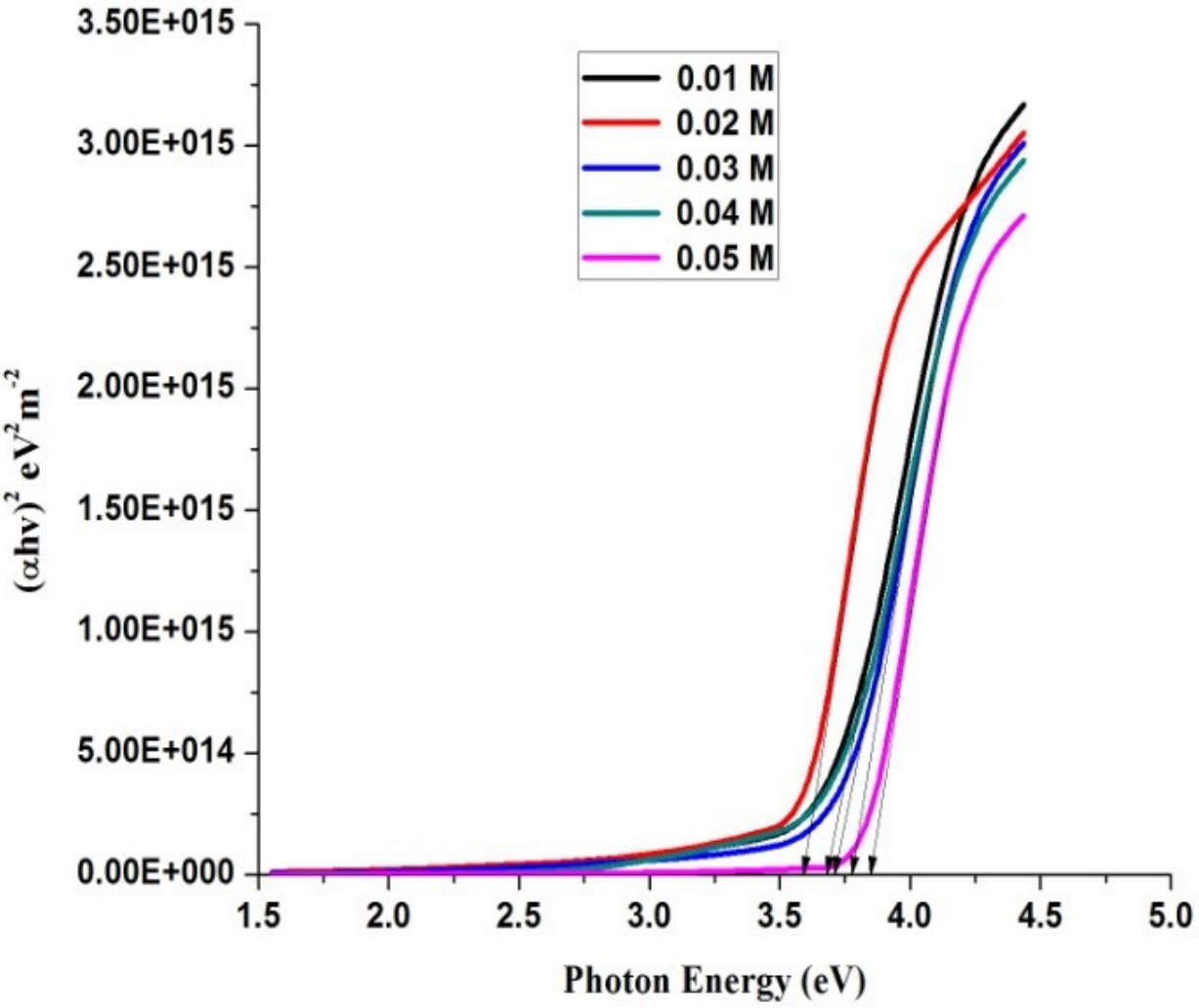

Figure 3. Band gap energies for different molar concentrations of cobalt.

3. Results and discussions

3.1 Optical characterization

The absorptions at different molar concentrations of the cations are presented in Figure 2. Optical range covered is 200 nm to 800 nm.

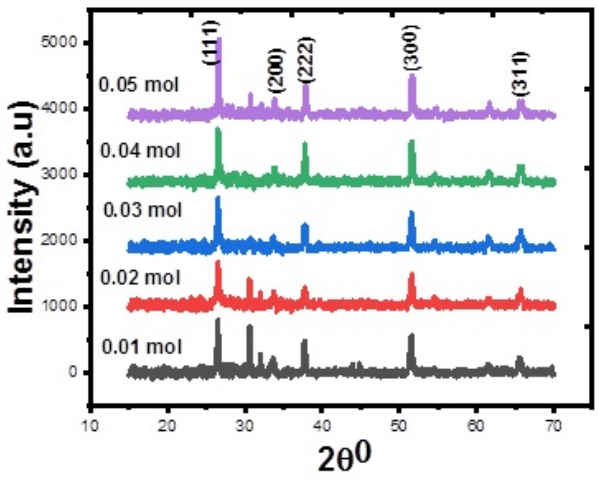

Figure 4. XRD spectra for all varied concentrations of cobalt.

The absorption spectra decreased steadily as they progressed from the ultraviolet (UV) region to the visible region, indicating band to band transition of the cobalt oxide films. Increased molar concentration from 0.01 to 0.04 M shows a closely packed spectrum within the UV region. From SEM analysis, these closed-packed spectrum is porous (contains pores). These pores on the film's surface aid in trapping the UV light, hence can store the UV radiation in the material. Such ability indicates that cobalt oxide cell can act as a good storage material for photovoltaics. A further increment in molar concentration to 0.05 mol resulted in a band edge shift from higher wavelength to lower wavelength (blue shift). The observed blue shift for the band edge is a consequence of widened band gap and higher concentration effect.

Figure 3 displays the band gap energies for varied concentrations of cobalt.

Tauc's plot was used to obtain the band gap values at different molar concentrations (Figure 3). The band gap values (3.65 eV to 3.85 eV) in this research are greater than the value (2.4 eV) for the bulk phase of CoO. This increase in

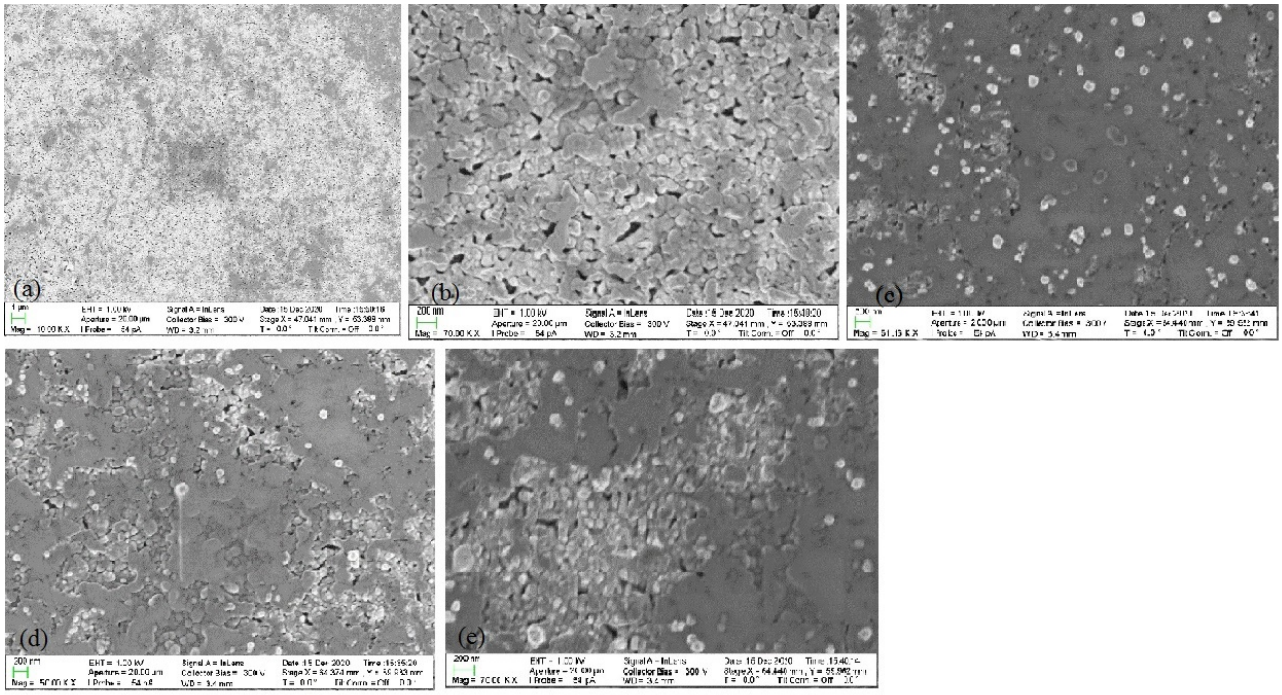

Figure 5. SEM image of CoO deposited at (a) 0.01 mol, (b) 0.02 mol, (c) 0.03 mol, (d) 0.04 mol and (e) 0.05 mol.

band gap can be likened to higher concentration effect and quantum-size phenomenon. The quantum-size phenomenon results in a blue-shift and subsequently shifts the band gap to higher energies [13]. For semiconductor particles in the nano-range, an increase in band gap results in a blue-shift [14]. Depending on the molarity concentration, the highest band gap was obtained at 0.05 M. The results obtained in this research find perfect agreement with previous reports of [14, 15].

3.2 Structural characterization

The XRD spectra for all varied concentrations are displayed in Figure 4. The observed XRD patterns for all concentrations appear identical; as such, no additional peaks are evident, indicating the non-existence of any impurity phase. Thus, at higher concentrations, the results show that the overall crystalline structure of the studied films remains unchanged. From Figure 3, well-defined peaks are evident, suggesting the crystalline nature of the films. The observed peaks are positioned at 2θ values of 29.12^o, 31.59^o, 48.03^o, 56.47^o and 66.21^o corresponding to crystal planes of [111], [200], [222], [300] and [311] which are consistent with the cubic structure. The [111] plane appears to be the preferred growth plane. This result agrees with previous reports [15–19].

The crystallite sizes (in nm) in this research were calculated from Debye-Scherrer's equation [20] using the expression:

$$D = \frac{K\lambda}{\beta \cos\theta}$$

The films have crystallite sizes within the range of 0.7 nm to 1 nm for different molar concentrations of cobalt.

The dislocation density was between 3.09 m^2 to 6.45 m^2.

The SEM images of the films are displayed in Figure 5(a-e). The crystallites are spread across the surface of the films. From Figure 5(b), the SEM image of the film obtained at 0.02 mol appears porous. However, at increased molarity (0.03 mol, 0.04 mol, 0.05 mol), the porosity of the material appears reduced as the films were observed to be more compacted resulting in lower particle sizes distributed on the surface of the films. Similar CoO with porous morphology has been reported [21]. The porous nature provides the films with the advantage of absorbing UV light, which is a very good requirement for absorber materials for solar cells

Table 2. Resistivity, conductivity and thickness values for CoO .

Samples	Thickness, t(nm)	Resistivity,ρ (Ω.cm)	Conductivity, σ $(\Omega.cm)^{-1}$
0.01 mol	108.86	5.121×10^{-11}	1.952×10^{10}
0.02 mol	110.93	5.242×10^{-11}	1.907×10^{10}
0.03 mol	111.72	6.412×10^{-11}	1.559×10^{10}
0.04 mol	113.06	6.512×10^{-11}	1.535×10^{10}
0.05 mol	117.73	7.127×10^{-11}	1.403×10^{10}

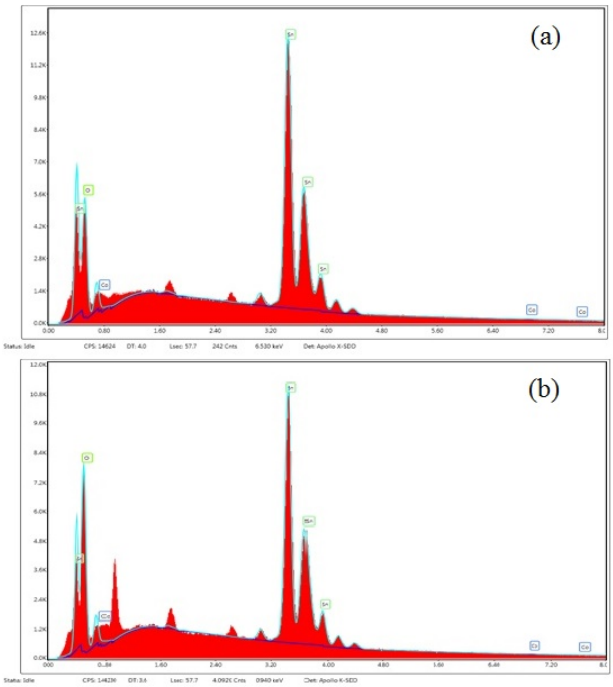

Figure 6. EDX spectrum of CoO deposited at (a) 0.02 mol, (b) 0.05 mol.

fabrication.
The elemental composition of the grown CoO films obtained by EDX analysis is displayed in Figures 6(a) and 6(b).
The EDX spectrum for the films shows peaks corresponding to cobalt and oxygen respectively confirming the growth of CoO.

3.3 Electrical studies

The electrical characterizations were measured using four-point probe (Model T345). The plot of the values of resistivity versus film thickness is presented in Figure 7.
The electrical properties of CoO thin films revealed that the material deposited at different molar concentrations of 0.01 mol, 0.02 mol, 0.03 mol, 0.04 mol and, 0.05 mol had thickness increment from $108.86 - 117.73$ nm with a corresponding increase in the resistivity of the deposited material from $5.121 \times 10^{-11} - 7.127 \times 10^{-11}$ (Ω.cm) which resulted in a decrease of the electrical conductivities of the deposited material from $1.952 \times 10^{10} - 1.403 \times 10^{10}$ $(\Omega.\text{cm})^{-1}$ (Table 2). The increased resistivity stems from reduction in the mean free path of the conduction electrons arising from increase in scattering effect. Conduction electrons (CEs) are responsible for the conductivity of any material. If the CEs are free to move within the lattice, conductivity becomes easier, if not mobile, conductivity is unlikely. In every material, the CEs are attached to the atoms in the form of covalent bonding. However, once the electrons gain enough energy, they easily break the covalent bond and are free to move within the lattice. The movement of these free electrons result in the material's conductivity. Therefore, the implication of high resistivity at increased molar concentration is that the material's conductivity is reduced because this high resistivity prevents the electrons from easily breaking up the covalent bond, thus slowing down conductivity.

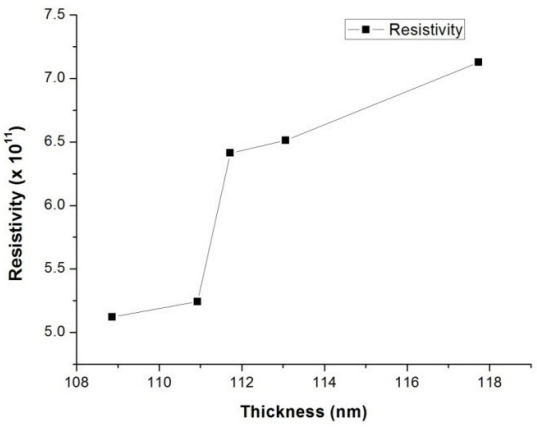

Figure 7. Electrical resistivity versus thickness of CoO for different molar concentrations.

4. Conclusion

Cobalt oxide films were deposited on FTO glass substrates at different molar concentrations by electrodeposition. The characterized films were studied for their optical, morphological, structural and electrical properties. The optical and morphological results indicate closely packed spectrum having pores on the surface of the material. These pores are capable of trapping UV radiation, thus suggesting the material's usefulness as an absorber for solar cell fabrication. Structural (XRD) studies suggest the grown films are crystalline, belonging to the cubic crystal structure. The crystallite sizes were calculated from Debye-Scherrer's equation and found to have values between 0.7 nm and 1 nm for different molar concentrations of cobalt. The electrical studies reveal increase in resistivity and decrease in conductivity as thickness and molarity increases. The increased resistivity in response to increased thickness and increased molar concentration were observed to have occurred due to the reduction in the mean free path of the CEs of cobalt oxide. Hence, cobalt oxide will function better as a conductive material at lower molar concentration.

Conflict of interest statement:
The authors declare that they have no conflict of interest.

References

[1] D. M. Jeroh, A. J. Ekpunobi, and D. N. Okoli. "Optical and structural characterization of CdSe:Eu at different volumes of europium concentration". *Journal of Theoretical and Applied Physics*, **16**:1, 2022.

[2] A. I. Hassan and S. I. Maki. "Structural and optical properties of copper- doped cobalt Oxide thin films prepared by spray pyrolysis". *Int. J. Eng. Sci. Res. Technol.*, **6**:527, 2017.

[3] A. Lakehal, B. Bedhiaf, A. Bouaza, H. Benhebal, A. Ammari, and C. Dalache. "Structural, optical and

electrical properties of Ni-doped Co_3O_4 prepared via sol-gel technique". *Mater. Res.*, **21**:1, 2018.

[4] L. Nikzad, M. R. Vaezi, and S. Alibeigi. "Preparation of cobalt oxide/zinc oxide nanocomposite". *IJE Transactions B: Applications*, **23**:133, 2010.

[5] S. N. F. Moridon, M. N. I. Salehmin, K. Arifin, L. F. Minggu, and M. B. Kassim. "Synthesis of cobalt oxide on FTO hydrothermal method for photoelectrochemical water splitting application". *Appl. Sci.*, **11**:3031, 2021.

[6] M. M. Rahman, H. A. Miran, Z. T. Jiang, M. Altarawneh, L. S. Chuah, H. L. Lee, A. Amri, N. Mondinos, and B. Z. Dlugogorski. "Investigation of the post-annealing electromagnetic response of Cu–Co oxide coatings via optical measurement and computational modelling". *RSC Adv.*, **7**:16826, 2017.

[7] L. Kelpsaite, J. Baltrusaitis, and E. Valatka. "Electrochemical deposition of porous cobalt oxide films on AISI 304 type steel". *Mater. Sci.*, **17**:236, 2011.

[8] I. Barauskiene and E. Valatka. "Electrocatalytic and pseudocapacitive properties of cobalt (hydro) oxide films on sintered metal fiber filter". *Materials for Renewable and Sustainable Energy*, **7**:1, 2018.

[9] M. Mirzaeian, N. Akhanova, M. Gabdullin, Z. Kalkozova, A. Tulegenova, S. Nurbolat, and K. Abdullin. "Improvement of the pseudocapacitive performance of cobalt oxide-based electrodes for electrochemical capacitors". *Energies*, **13**:1, 2020.

[10] M. Zahan and J. Podder. "Surface morphology, optical properties and Urbach tail of spray deposited Co_3O_4 thin films". *J. Mater. Sci.: Mater. Electron.*, **30**:4259, 2019.

[11] I. M. Dharmadasa and J. Haigh. "Strengths and Advantages of Electrodeposition as a Semiconducto Growth Technique for Applications in Macroelectronic Devices". *J. Electrochem. Soc.*, **153**:G47, 2006.

[12] K. A. Urazov, V. I. Yaskevich, and B. E. Myrzabekov. "Electrochemical deposition of $Cu_2ZnSnSe_4$ thin films on Mo-glass electrode from tartaric acid". *Int. J. Electrochem. Sci.*, **17**:1, 2022.

[13] D.M. Jeroh, A.J. Ekpunobi, and D.N. Okoli. "The optical properties of europium-doped zinc selenide films". *Journal of Nano- and Electronic Physics*, **12**:05006, 2020.

[14] C. R. Dhas, R. Venkatesh, K. Jothivenkatachalam, A. Nithya, B. S. Benjamin, A. M. E. Raj, K. Jeyadheepen, and C. Sanjeeviraja. "Visible light driven photocatalytic degradation of Rhodamine B and Direct Red using cobalt oxide nanoparticles". *Ceramics International*, **41**:9301, 2015.

[15] S. Farhadi, M. Javanmard, and G. Nadri. "Characterization of cobalt oxide nanoparticles prepared by the thermal decomposition of $[Co(NH_3)_5(H_2O)](NO_3)_3$ complex and study of their photocatalytic activity". *Acta Chim. Slov.*, **63**:335, 2016.

[16] P. Prieto, J. F. Marco, A. Serrano, M. Manso, and J. de la Figuera. "Highly oriented (111) CoO and Co_3O_4 thin films grown by ion beam sputtering". *J. Alloy. Compd.*, **810**:151912, 2019.

[17] V. Helen and P. J. Joseph. "Influence of annealing on the structural, optical and magnetic properties of CoO thin films". *J. Mater. Res. Innov.*, **23**:200, 2017.

[18] Z. N. Kayani, S. Arshad, S. Riaz, R. Zia, and S. Naseem. "Structural characterization and optical properties of cobalt oxide thin films.". *The 2014 world congress on Advanced in Civil, Environmental and Materials Research, Busan, Korea*, :1, 2014.

[19] D. U. Onah, C. E. Okeke, R. U. Osuji, B. A. Ezekoye, J. E. Ekpe, G. F. Ibeh, A. B. C. Ekwealor, and F. I. Ezema. "Study of the effects of thermal annealing on the optical band gap of nanocrystalline CoO thin films prepared by chemical bath deposition". *Chem. Mater. Res.*, **3**:43, 2013.

[20] S. M. Jogade, D. S. Sutrave, and S. D. Gothe. "Electrochemical analysis of cobalt oxide thin film for supercapacitor". *Int. J. Adv. Res. Phys. Sci.*, **2**:36, 2015.

[21] E. Amin-Chalhoub, T. Duguet, D. Samelor, O. Debieu, E. Ungureanu, and C. Vahlas. "Constantin chemical vapour deposition of low reflective cobalt (II) oxide films". *Appl. Surf. Sci.*, **360**:540, 2016.